

# 1 Assessing the role of rare pathogenic variants in heart 2 failure progression by exome sequencing in 8,089 patients

3  
4 Olympe Chazara<sup>1</sup>, Marie-Pierre Dubé<sup>2,3,4</sup>, Quanli Wang<sup>1</sup>, Lawrence Middleton<sup>1</sup>, Dimitrios Vitsios<sup>1</sup>,  
5 Anna Walentinsson<sup>5</sup>, Qing-Dong Wang<sup>6</sup>, Kenny M. Hansson<sup>6</sup>, Christopher B. Granger<sup>7</sup>, John  
6 Kjekshus<sup>8</sup>, Carolina Haefliger<sup>1</sup>, Jean-Claude Tardif<sup>2,3</sup>, Dirk S. Paul\*<sup>1</sup> and Keren Carss\*<sup>1</sup>

7  
8 <sup>1</sup>Centre for Genomics Research, Discovery Sciences, BioPharmaceuticals R&D, AstraZeneca, Cambridge, UK; <sup>2</sup>Montreal  
9 Heart Institute, Montreal, Canada; <sup>3</sup>Université de Montréal, Faculty of Medicine, Department of Medicine, Université de  
10 Montréal, Montreal, Canada; <sup>4</sup>Université de Montréal Beaulieu-Saucier Pharmacogenomics Centre, Montreal, Canada;  
11 <sup>5</sup>Translational Science & Experimental Medicine, Research and Early Development, Cardiovascular, Renal and Metabolism  
12 (CVRM), BioPharmaceuticals R&D, AstraZeneca, Gothenburg, Sweden; <sup>6</sup>Bioscience Cardiovascular, Research and Early  
13 Development, Cardiovascular, Renal and Metabolism (CVRM), BioPharmaceuticals R&D, AstraZeneca, Gothenburg,  
14 Sweden; <sup>7</sup>Duke Clinical Research Institute, Duke University, Durham, North Carolina; <sup>8</sup>Department of Cardiology,  
15 University of Oslo, Oslo, Norway; \*These authors contributed equally.

16 Correspondence: Dirk S. Paul, [dirk.paul@astrazeneca.com](mailto:dirk.paul@astrazeneca.com)

## 19 Abstract

20  
21 Most therapeutic development is targeted at slowing disease progression, often long after the initiating  
22 events of disease incidence. Heart failure is a chronic, life-threatening disease and the most common  
23 reason for hospital admission in people over 65 years of age. Genetic factors that influence heart  
24 failure progression have not yet been identified. We performed an exome-wide association study in  
25 8,089 patients with heart failure across two clinical trials, CHARM and CORONA, and one  
26 population-based cohort, the UK Biobank. We assessed the genetic determinants of the outcomes  
27 ‘time to cardiovascular death’ and ‘time to cardiovascular death and/or hospitalisation’, identifying  
28 seven independent exome-wide-significant associated genes, *FAM221A*, *CUTC*, *IFIT5*, *STIMATE*,  
29 *TAS2R20*, *CALB2* and *BLK*. Leveraging public genomic data resources, transcriptomic and pathway  
30 analyses, as well as a machine-learning approach, we annotated and prioritised the identified genes for  
31 further target validation experiments. Together, these findings advance our understanding of the  
32 molecular underpinnings of heart failure progression and reveal putative new candidate therapeutic  
33 targets.

## 35 Introduction

36

37 Heart failure is a common, chronic health condition with increasing prevalence. In 2017, an estimated  
38 64.3 million people worldwide were living with heart failure<sup>1</sup>. Around 2% of adults have heart failure  
39 and, in those over the age of 65, the prevalence increases to 6–10%<sup>2-5</sup>. Although survival after  
40 diagnosis has improved, death rates remain high, with 5-year survival averaging 50%<sup>6</sup>. Heart failure is  
41 the leading cause of both hospitalization and readmission amongst older adults<sup>7-9</sup>.

42 Studies have estimated the heritability of heart failure at 26%<sup>10</sup>. Genome-wide association studies  
43 (GWAS) have characterised the contribution of common genetic variants to the aetiology of heart  
44 failure<sup>11-13</sup>. We recently described the distinct contribution of rare genetic variation to all-cause heart  
45 failure in a case-control study<sup>14</sup>. We also investigate the genetic differences between heart failure  
46 subtypes based on left ventricular ejection fraction (LVEF) and the burden of Mendelian  
47 cardiomyopathy variants in these patients. We observed an enrichment of variants typically associated  
48 with dilated cardiomyopathy in patients with ischemic heart failure, in particular, protein-truncating  
49 variants in the *TTN* gene. Our data supported the notion that genes linked to Mendelian  
50 cardiomyopathy could represent therapeutic targets for a broader heart failure indication. Collectively,  
51 the vast majority of genetic studies for common chronic diseases such as heart failure have informed  
52 on disease incidence, with an unclear relationship to disease progression.

53 Most therapeutic development is targeted at slowing or arresting disease progression in individuals  
54 who already have disease. However, studies of disease progression remain challenging, as they require  
55 extensive, longitudinal clinical data that require expert curation, such as diagnoses, hospitalisation  
56 dates, causes of hospitalisation and death. They also present statistical and computational challenges,  
57 as the most well-known approach for analysis of survival (or time-to-event) analysis, the Cox  
58 proportional hazards model<sup>15</sup>, does not scale well to large datasets<sup>16</sup>. Partially overcoming these  
59 challenges, powerful and efficient time-to-event analysis frameworks have recently been applied to the  
60 UK Biobank<sup>17-19</sup>. For heart failure, these studies have mostly focused on time-to-diagnosis phenotypes  
61 and/or considered only common genetic variants<sup>20</sup>.

62 The aim of this study was to identify rare variants associated with heart failure progression. Rare  
63 variants have typically larger effects on phenotypes and reveal more direct insights into biology that  
64 can be exploited for medicine development<sup>21</sup>. Specifically, the objectives of this study were to (1)  
65 perform a survival analysis of heart failure patients to identify genes with an excess or depletion of  
66 rare variants in individuals with a detrimental outcome such as shorter time to cardiovascular death;  
67 (2) explore how these results can inform the genetic architecture of heart failure progression; and (3)  
68 evaluate which of the identified progression-associated candidate genes could present potential  
69 candidates for therapeutic development. To address these objectives, we analysed whole-exome  
70 sequencing data from patients with heart failure, representing all broad clinical subtypes, from the  
71 Candesartan in Heart Failure-Assessment of Reduction in Mortality and Morbidity (CHARM) and

72 Controlled Rosuvastatin Multinational Trial in Heart Failure (CORONA) clinical trials, and heart  
73 failure patients from the UK Biobank<sup>22-24</sup>. All three cohort studies had extensive clinical information  
74 available and had been previously studied for heart failure incidence. We applied gene-based  
75 collapsing analyses within each study, followed by meta-analysis to discover genes with an excess of  
76 rare variants associated with two heart failure outcomes, ‘time to cardiovascular death’ and ‘time to  
77 cardiovascular death and/or hospitalisation’.

78  
79

## 80 **Results**

81

82 **Description of the study cohorts and analytical approach.** In this study, we analysed a total of  
83 8,089 heart failure patients: 2,672 from CHARM, 2,776 from CORONA and 2,641 from the UK  
84 Biobank. From these 8,089 individuals, 1,328 (16.4%) died of cardiovascular death, and 2,451  
85 (30.3%) either died of cardiovascular death or were hospitalised due to heart failure following study  
86 entry (**Table 1, Figure 1**).

87 First, we analysed the three study cohorts separately to detect rare variants associated with the two  
88 outcomes ‘time to cardiovascular death’ and ‘time to cardiovascular death and/or heart failure  
89 hospitalisation’. We used gene-level collapsing analyses to classify the genotypes, and Cox  
90 proportional hazards regression with Firth’s penalized likelihood to analyse each individual’s disease  
91 progression (**Methods**). In gene-level collapsing analyses, the proportion of cases with a qualifying  
92 variant is compared with the proportion of controls with a qualifying variant in each gene. We applied  
93 ten different sets of qualifying variant filters (models) (**Methods**). Finally, we used a meta-analysis  
94 approach to identify genes with overall evidence of association.

95

96 **Rare-variant analysis for time to cardiovascular death in heart failure patients.** For time to  
97 cardiovascular death in heart failure patients, the gene-based collapsing meta-analysis identified five  
98 significantly associated genes ( $p < 2 \times 10^{-7}$ ): *FAM221A* ( $p = 3.85 \times 10^{-8}$ , hazard ratio (HR) 5.14), *CUTC*  
99 ( $p = 3.90 \times 10^{-8}$ , HR 5.13), *IFIT5* ( $p = 4.77 \times 10^{-8}$ , HR 4.77), *STIMATE* ( $p = 7.68 \times 10^{-8}$ , HR 4.39) and  
100 *TAS2R20* ( $p = 2.57 \times 10^{-7}$ , HR 3.93) (**Table 2, Figure 2A-E**). The meta-analysis for these five genes was  
101 based on the survival analysis of the three contributing studies, with at least five carriers per study.  
102 None of the single-study analysis results for time to cardiovascular death in heart failure patients  
103 passed the significance threshold of  $p < 2 \times 10^{-7}$ , demonstrating the power of meta-analysis for this  
104 phenotype to discover novel rare-variant based signals (**Supplementary Tables 1-3**). The meta-  
105 analysis also revealed a significant association for *CHRNA9* ( $p = 1.89 \times 10^{-7}$ , HR 4.72) but the supporting  
106 survival analysis in CHARM was violating the proportionality hazard assumption; therefore, we did  
107 not report this association result.

108 We assessed the distributions of the qualifying variants along the length of each of the five  
109 identified genes (**Figure 3A-E**). We found that the observed associations with the lowest p-values  
110 were driven by at least eight variants per gene, and were evenly distributed across the length of the  
111 gene sequence (**Supplementary Table 4**).

112

113 **Rare-variant analysis for the composite of time to cardiovascular death and/or heart failure**  
114 **hospitalisation.** For the second of the two outcomes investigated, the composite of time to  
115 cardiovascular death and/or heart failure hospitalisation, the gene-based collapsing meta-analysis  
116 identified two significantly associated genes ( $p < 2 \times 10^{-7}$ ): *CALB2* ( $p = 4.82 \times 10^{-9}$ , HR 4.47) and *BLK*  
117 ( $p = 5.46 \times 10^{-8}$ , HR 6.91) (**Table 2, Figure 2F-G**). While the meta-analysis for *CALB2* result was based  
118 on the survival analysis of the three studies, with at least five carriers per study, the result for *BLK* was  
119 only based on the CORONA and UK Biobank studies, as there was only one carrier for *BLK* in  
120 CHARM. The proportionality hazard assumption was not met for *CALB2* in CHARM, but after  
121 removal of the study from the analysis, the meta-analysis result remained significant ( $p = 2.15 \times 10^{-8}$ , HR  
122 5.48).

123 We report one significant result from the single-study analysis for time to cardiovascular death  
124 and/or heart failure hospitalisation in heart failure patients: *RAD54L* in the flexible non-synonymous  
125 model in CHARM ( $p = 6.64 \times 10^{-8}$ , HR 3.96; **Supplementary Tables 5-7**). *RAD54L* in the  
126 corresponding analysis in CORONA and the UK Biobank was not significantly associated with heart  
127 failure progression ( $p > 0.1$  and number of qualifying variant carriers  $> 30$  in both cohorts). Different  
128 genetic architecture across the studies could reflect underlying clinical differences, due to the differing  
129 recruitment criteria employed.

130 We assessed the distributions of the qualifying variants along the length of the identified genes  
131 (**Figure 3F-G**) and found that the observed associations with the lowest p-values were driven by 13  
132 variants for the *CALB2* gene and seven variants for *BLK* (**Supplementary Table 4**). We found these  
133 variants to be evenly distributed across the length of the gene sequence (**Supplementary Table 4**).

134

135 **Orthogonal genetic evidence in support of rare-variant meta-analysis results.** To investigate to  
136 what extent the discovered genes from our rare-variant meta-analyses are associated with related  
137 phenotypes in complementary data sources, we annotated the genes with orthogonal genetic evidence:  
138 (1) curated common-variant association studies for cardiovascular diseases from the Cardiovascular  
139 Disease Knowledge Portal (<https://cvd.hugeamp.org/>); (2) known Mendelian cardiomyopathy-causing  
140 genes; and (3) a gene prioritisation method that leverages external data sources using a machine-  
141 learning (ML) approach (Mantis-ML)<sup>25</sup>.

142 We collated the curated evidence from published GWAS from the Cardiovascular Disease  
143 Knowledge Portal for the seven candidate genes from the meta-analysis for both tested outcomes  
144 (**Table 3**). We found genome-wide significant associations with cardiovascular traits in the genomic

145 regions of *CUTC*, *IFIT5*, *STIMATE*, *CALB2* and *BLK*. There were also genome-wide significant  
146 associations with lipids traits in the regions of *CUTC*, *STIMATE*, *CALB2* and *BLK*, and with  
147 anthropometric traits in the regions of *FAM211A*, *CUTC*, *STIMATE*, *CALB2* and *BLK* (**Table 3A**). A  
148 limitation of this comparison is that a majority of the reported associations had the UK Biobank  
149 included in the meta-analysis, and the relationship between the GWAS index variants and causal genes  
150 at the loci requires further experimental confirmation. However, we did not detect genome-wide  
151 significant associations in either the region or the gene for the most relevant reported phenotypes, i.e.,  
152 heart failure, non-ischemic cardiomyopathy, atrial fibrillation, any cardiovascular disease, myocardial  
153 infarction, and hypertension. Only *IFIT5*, *STIMATE* and *CALB2* had suggestive associations ( $p < 1 \times 10^{-5}$ )  
154 for any cardiovascular disease (*IFIT5* and *STIMATE*) or hypertension (*STIMATE* and *CALB2*)  
155 (**Table 3B**). The lowest p-values observed in the *CUTC* region were for heart rate ( $p = 2.73 \times 10^{-9}$ ),  
156 height ( $p = 1.80 \times 10^{-28}$ ) and atrial fibrillation ( $p = 1.79 \times 10^{-4}$ ) (**Table 3B**).

157 Among the known rare or low-frequency variants in cardiomyopathy-causing genes previously  
158 identified such as *TTN*, *MYH7* and *MYBPC3* for heart failure incidence and *LMNA* and *LAMP2* for  
159 heart failure progression, we observed a non-significant association of ultra-rare variants in *MYBPC3*  
160 with time to cardiovascular death ( $p = 2.05 \times 10^{-6}$ , HR 4.38), but not for the other reported genes. Most of  
161 these cardiomyopathy-causing genes had a very low number of pathogenic variant carriers, making  
162 interpretation challenging. However, *TTN* pathogenic variants were more frequent, indicating that *TTN*  
163 might be specifically associated with heart failure incidence rather than progression, which has been  
164 reported previously<sup>26</sup>.

165 Finally, we applied Mantis-ml, a ML framework leveraging publicly available gene annotation data  
166 to prioritise disease-gene associations<sup>25</sup>. We used this orthogonal method to investigate the extent to  
167 which the significant genes from our rare-variant meta-analyses ( $p < 0.01$ ) are similar to genes known,  
168 or predicted with high confidence, to be associated with relevant phenotypes (i.e., the top-ranked  
169 genes from Mantis-ml conditioned on heart failure or cardiomyopathy). These similarities were  
170 quantified using a step-wise hypergeometric test (**Methods**). For both outcomes, we found the overlap  
171 in relevant phenotypes to be greater for the qualifying variant models that capture functional variants  
172 than for the synonymous negative control model (**Supplementary Figs. 1A, 1B**). In addition,  
173 collapsing the 33 heart failure/cardiomyopathy disease classes available to a single metric (i.e., taking  
174 either the maximum or the AUC), we found significantly superior performance of the pooled  
175 qualifying variant model compared to the synonymous model for both, time to cardiovascular death  
176 ( $p_{\max} = 1.6 \times 10^{-5}$  and  $p_{\text{AUC}} = 8.0 \times 10^{-4}$ ) and time to cardiovascular death and/or hospitalisation for heart  
177 failure ( $p_{\max} = 5.1 \times 10^{-5}$  and  $p_{\text{AUC}} = 3.9 \times 10^{-4}$ ) (**Supplementary Fig. 1C**). Taken together, these results  
178 showed that the features of the most significantly associated genes from our meta-analysis share  
179 similarities with the features of genes already known, or strongly predicted, to be associated with  
180 relevant phenotypes, supporting our genetic data.

181

182 **Expression analysis in heart tissues aids gene prioritisation for further validation.** Next, we  
183 assessed the expression patterns of the candidate causal genes underlying the genetic associations for  
184 heart failure progression. Normalized gene expression data collected by the GTEx Project<sup>27</sup> were  
185 interrogated for the seven candidate genes from the meta-analysis for both tested outcomes (**Table 2**).  
186 We used the 54 different tissues sampled by GTEx as well as a subset of 16 cardiovascular tissues.

187 The overall tissue expression analysis revealed that *CUTC*, *STIMATE* and *IFIT5* are expressed in  
188 almost all tissues analysed; *CALB2* and *BLK* are expressed in multiple tissues but not all; and  
189 *TAS2R20* and *FAM221A* have comparatively low expression across all tissues analysed  
190 (**Supplementary Fig. 2A**). *CUTC* was the gene most strongly expressed in the heart. In cardiovascular  
191 tissue, a similar gene grouping was observed, with *CUTC* highest in skeletal muscle, *CALB2* in  
192 adipose, and *BLK* in whole blood and spleen tissues (**Supplementary Fig. 2B**).

193 Next, we analysed differential expression of the candidate genes in tissues from ventricular  
194 myocardial biopsies in heart failure with preserved/reduced ejection fraction (HFpEF/HFrEF),  
195 (idiopathic) dilated cardiomyopathy (DCM), hypertrophic cardiomyopathy (HCM), ischemic  
196 cardiomyopathy (ICM), and controls from three separate public transcriptomics studies (**Figure 4**,  
197 **Supplementary Table 8**)<sup>28</sup>. *CUTC*, *IFIT5*, *TAS2R20*, *FAM221A* and *BLK* showed significant  
198 differential expression between the healthy and diseased heart. Among these, *CUTC* was most  
199 consistently dysregulated, being downregulated across studies and heart failure aetiologies. *TAS2R20*  
200 and *BLK* have low expression in the heart, making the results challenging to interpret. *FAM221A*,  
201 *IFIT5* and *TAS2R20* showed significant differential expression between HFpEF vs HFrEF patients in  
202 the right ventricle (**Figure 4, Supplementary Fig. 2, Supplementary Table 8**).

203 Taken together, based on all transcriptional datasets, we highlight *CUTC* as a potential therapeutic  
204 target for heart failure progression that warrants further experimental validation and assessment.

205

206 **Functional enrichment analysis identifies molecular functions and pathways of candidate genes.**

207 To identify potential molecular functions and pathways underlying the genetic associations, we  
208 performed a gene ontology analysis of the candidate genes. We tested 1298 unique genes ranked by  
209 their lowest fixed model p-value across the ten non-synonymous collapsing analysis models from the  
210 time to cardiovascular death meta-analysis. We found enrichment (adjusted  $p < 0.05$ ) for the following  
211 molecular functions: adenylyl ribonucleotide binding (GO:0032559,  $p = 8.91 \times 10^{-4}$ ); adenylyl nucleotide  
212 binding (GO:0030554,  $p = 1.43 \times 10^{-3}$ ); lamin binding (GO:0005521,  $p = 1.49 \times 10^{-3}$ ); among others  
213 (**Supplementary Fig. 3A, Supplementary Table 9**).

214 We also performed the analysis for the 956 unique genes from the time to cardiovascular death  
215 and/or hospitalisation for heart failure meta-analysis. This analysis revealed enrichment for the  
216 following molecular functions and biological pathways: ion binding (GO:0043167,  $p = 3.42 \times 10^{-3}$ );  
217 glycine, serine and threonine metabolism (KEGG:00260,  $p = 4.17 \times 10^{-3}$ ); among others  
218 (**Supplementary Fig. 3B, Supplementary Table 9**).

219

## 220 Discussion

221

222 The identification of determinants of disease progression is critical for drug development, as most  
223 clinical trials assess the efficacy and safety of treatments that slow or arrest disease progression in  
224 patients with disease or prevent secondary events in specific patient groups. However, in contrast to  
225 the relatively large number of genetic studies on the incidence of common chronic diseases, including  
226 heart failure, there are few published studies investigating the genetic basis of disease progression.

227 In our study, we implemented a survival analysis for rare variants based on collapsing analysis and  
228 Cox proportional hazards regression with Firth's penalized likelihood. We analysed the whole-exome  
229 sequencing data of 8,089 heart failure patients from three clinically well-defined studies: two clinical  
230 trials, CHARM and CORONA, and one population-based study: the UK Biobank. We performed  
231 meta-analysis and reported results found in at least two studies and supported by at least five carriers  
232 per study. We report seven genes not previously associated with heart failure progression with hazard  
233 ratios between 3.93 and 6.91. Specifically, we identified five candidate genes for cardiovascular death  
234 risk in heart failure patients: *FAM221A*, *CUTC*, *IFIT5*, *STIMATE* and *TAS2R20*, and two candidate  
235 genes for the composite of cardiovascular death and/or heart failure hospitalisation risk in heart failure  
236 patients: *CALB2* and *BLK*.

237 Importantly, none of these identified candidate gene loci have previously been associated with  
238 heart incidence through common-variant association studies, suggesting distinct genetic aetiology for  
239 heart failure progression compared to incidence. However, when evaluating the prior evidence of  
240 association with disease incidence, we found that all but two candidate gene loci (i.e., *FAM221A* and  
241 *TAS2R20*) harboured genome-wide significant, common-variant associations with cardiovascular  
242 traits, including heart rate, ascending aorta diameter and blood pressure.

243 We showed that several of the candidate genes are expressed in relevant cardiovascular tissues. In  
244 particular, *CUTC* is expressed strongly in heart tissues. Using heart single-cell RNA-seq data, we  
245 demonstrated that *CUTC* is expressed by all cardiac cell types with highest fractional expression in  
246 cardiomyocytes (**Supplementary Fig. 4**). Further, we demonstrated differential expression of five out  
247 of seven candidate genes between diseased and healthy hearts and/or between heart failure subtypes.

248 Finally, ML-based enrichment analysis supported our gene ranking from the meta-analysis,  
249 especially for the cardiovascular death outcome, as indicated by step-wise hypergeometric analyses.  
250 Functional enrichment analysis highlighted known pathways in cardiovascular disease, such as lamin  
251 binding (enrichment supported by *SUN1*, *TMEM201*, *SUN2*, *SYNE1* and *PLCB1*), and novel pathways,  
252 such as glycine, serine and threonine metabolism (supported by *GLDC*, *PGAM1* and *ALDH7A1*)<sup>29,30</sup>.

253 *CUTC* was the only gene that showed an association with both tested endpoints, as well as strong  
254 expression in the heart and differential expression between diseased and healthy heart tissues. *CUTC*  
255 encodes a member of the CUT family of copper transporters that are associated with copper

256 homeostasis and involved in the uptake, storage, delivery and efflux of copper<sup>31-33</sup>. Defective copper  
257 metabolism has been linked to various cardiovascular diseases, including heart failure. Mutations in  
258 genes encoding copper chaperones/transporters associate with cardiac disease in humans and mice<sup>34</sup>.  
259 Notably, the ongoing TRACER-HF trial (NCT03875183) evaluates the effects of a copper-binding  
260 agent INL1 in patients with HFrEF. INL1 is hypothesized to redistribute copper from high-  
261 concentration gradient (e.g., the circulation) to copper-depleted tissues (e.g., ischemic myocardial  
262 tissue), inducing heart regeneration. Although the exact function of CUTC remains to be determined,  
263 it has been suggested that it might act as an enzyme with Cu(I) as a cofactor rather than a copper  
264 transporter<sup>31</sup>. Moreover, CUTC participates in cardiac conduction and ion channel transport pathways  
265 based on the PathCards database (<https://pathcards.genecards.org>) and our co-expression network  
266 analysis suggested a role in muscle physiology and mitochondrial function (**Supplementary Fig. 4**).  
267 These pathways are all highly relevant biofunctions in heart failure pathophysiology. Our tractability  
268 assessment further revealed that CUTC contains a high-quality ligand pocket and is predicted  
269 druggable using small molecules (**Supplementary Table 10**). Taken together, *CUTC* may represent  
270 an attractive new candidate therapeutic target in heart failure.

271 Of note, alternative *CUTC* transcripts overlap *COX15*, encoding the Cytochrome C Oxidase  
272 Assembly Homolog. Despite a larger number of rare variant carriers than *CUTC*, *COX15* was not  
273 significantly associated with either cardiovascular death or the composite of cardiovascular death  
274 and/or heart failure hospitalisation in our analyses (**Supplementary Tables 11, 12**). Diseases  
275 associated with *COX15* include Mitochondrial Complex IV Deficiency, Nuclear Type 6 and Fatal  
276 Infantile Cardioencephalomyopathy Due To Cytochrome C Oxidase Deficiency. It has been proposed  
277 that *CUTC* and *COX15* functions in partnership as they share a bidirectional promoter<sup>35</sup>.

278 *STIMATE* and *CALB2* are involved in calcium binding, signalling or channel activity. Calcium  
279 pathways are fundamental for electrical signalling in the heart<sup>36</sup>. Several known mechanisms of  
280 cardiac pathologies are underlined by calcium channels<sup>36</sup>. A major class of drug targets already exist  
281 for calcium channel regulation<sup>37,38</sup>. Calcium antagonists have been used to treat ischemia, a common  
282 cause of heart failure<sup>39</sup>. *IFIT5* and *BLK*, are involved in immune system function. It is established that  
283 inflammation plays an important role in chronic heart failure, after myocardial infarction or other  
284 myocardial damage, and heart failure is associated with circulating inflammatory cytokines that can  
285 predict clinical outcomes<sup>40</sup>. Whether inflammation plays a causal role remains to be established<sup>41</sup>. A  
286 number of taste receptors including *TAS2R20* are expressed in human heart and the role of these  
287 receptor in cardiac physiology and pathophysiology is not well understood yet<sup>42</sup>. It is notable that  
288 *TAS2R20* RNA expression is significantly increased in the myocardium in HFpEF patients but not in  
289 HFrEF patients, suggesting that *TAS2R20* may have a specific role in HFpEF.

290 In our meta-analysis, we did not discover any significantly associated protective genes. Such genes  
291 would be particularly promising for drug development as a protective effect of loss of function mimics  
292 the therapeutic inhibition of a drug. We observed previously in genetic analyses of heart failure



293 incidence that detrimental association of rare variants are more prevalent than protective associations,  
294 because they are enriched for loss-of-function variants<sup>14</sup>.

295 We acknowledge that our study had limitations. Due to the paucity of exome-wide investigation of  
296 the role of rare variants in heart failure progression, we were currently unable to replicate our findings  
297 in an independent study cohort. More collaborative research is needed to address this limitation of our  
298 study, e.g., through the HERMES consortium that aims to assess the contribution of common genetic  
299 variants to heart failure progression<sup>20</sup>. Further, we note that the definition of heart failure amongst the  
300 cases was heterogeneous, for example, with respect to the presence or absence of cardiomyopathy, and  
301 different LVEF categories (HF<sub>r</sub>EF vs HF<sub>p</sub>EF). Due to the study of rare variants, stratifying patients  
302 according to phenotypic subtypes would have substantially reduced power. Additionally, for heart  
303 failure incidence and cardiomyopathy-associated rare variants, we previously detected some  
304 overlapping genetic architecture between heart failure subtypes<sup>14</sup>, supporting our combined approach  
305 in this study. Future larger studies would facilitate stratified analyses. Finally, our study focussed on  
306 individuals of European ancestry because there are insufficient numbers of patients of other ancestries.  
307 Further studies are needed to replicate our findings in other ancestry groups.

308 In conclusion, by rare-variant collapsing meta-analysis, we have identified seven candidate genes  
309 significantly associated with heart failure progression: *FAM221A*, *CUTC*, *IFIT5*, *STIMATE*, *TAS2R20*,  
310 *CALB2* and *BLK*. Pending replication, several of these genes could represent promising drug targets  
311 for heart failure, as supported by their tissue expression and function.

312

## 313 **Methods**

314

315 **Ethics statement.** Sites participating in the CHARM and CORONA studies received approval from  
316 local ethics committees for their conduct<sup>22,23</sup>. Only patients who gave written informed consent for  
317 genetic analysis and for whom a DNA sample was available were included in the present study. The  
318 present study was performed in accordance with the policies on bioethics and human biologic samples  
319 of AstraZeneca. The protocols for UK Biobank are overseen by the UK Biobank Ethics Advisory  
320 Committee. For more information see <https://www.ukbiobank.ac.uk/ethics/>.

321

322 **CHARM and CORONA studies.** The CHARM programme enrolled heart failure patients of >18  
323 years of age into three distinct trials and randomly assigned them to receive candesartan or placebo:  
324 patients with LVEF >40% (CHARM Preserved; NCT00634712); patients with LVEF ≤ 40% and  
325 treated with angiotensin converting enzyme inhibitor (CHARM Added; NCT00634309); and patients  
326 with LVEF ≤ 40% and intolerant to angiotensin-converting enzyme inhibitor treatment (CHARM  
327 Alternative; NCT00634400)<sup>22</sup>. In the CHARM study, heart failure cause could be defined as ischemic,  
328 idiopathic, hypertensive or other causes<sup>22</sup>. The CORONA study enrolled patients of >60 years of age  
329 with chronic heart failure of ischemic cause and a LVEF ≤ 40% and randomly assigned them to  
330 receive rosuvastatin or placebo (NCT00206310)<sup>23</sup>. An overview of the patient characteristics of the  
331 trials is provided in **Table 1**.

332 In the CHARM and CORONA trials, the same two endpoints (i.e., cardiovascular death and a  
333 composite of cardiovascular death and/or heart failure hospitalisation) were defined by the clinical  
334 teams. For CHARM, cardiovascular death or unplanned admission to hospital for the management of  
335 worsening congestive heart failure was the primary outcome for the trial. All deaths were classified as  
336 cardiovascular unless an unequivocal non-cardiovascular cause was established. An heart failure  
337 hospital admission was defined as an admission to hospital because of heart failure with evidence of  
338 worsening heart failure<sup>22</sup>. For CORONA, the primary outcome was death from cardiovascular causes,  
339 nonfatal myocardial infarction, or nonfatal stroke. Deaths were classified as due to cardiovascular  
340 causes unless a definite non-cardiovascular reason was identified. Hospitalization for heart failure  
341 required documentation that worsening heart failure was the principal reason for hospitalization<sup>23</sup>.

342

343 **UK Biobank.** The UK Biobank is a large prospective cohort study with 500,000 participants aged 40  
344 to 69 years recruited from the general population in the United Kingdom<sup>24</sup>. The UK Biobank ICD10  
345 codes (International Statistical Classification of Diseases and Related Health Problems, Tenth  
346 Revision codes) were interrogated for the following heart failure phenotypes: I11.0, I13.0, I13.2,  
347 I25.5, I42.0, I42.5, I42.8, I42.9 and I50.x<sup>11</sup>. Overall, 11,076 individuals with at least one primary or  
348 secondary hospital in-patient diagnoses code (Data-Field ID 41270), and/or at least one underlying  
349 (primary) cause of death in the death register (Data-Field ID 40001) in those categories, were

350 considered as heart failure patients. In order to more closely match a clinical study design, only cases  
351 with heart failure diagnosis codes dated prior to recruitment were included in the analyses.  
352 Measurements of LVEF were not performed for the UK Biobank patients, as it was only available for  
353 a small number of individuals randomly selected from the biobank (**Table 1**).

354 For our analysis, we defined two endpoints: cardiovascular death (CVD) and a composite of  
355 cardiovascular death and/or heart failure hospitalisation (CVD\_HFHOSP). In the UK Biobank,  
356 cardiovascular death was defined as a primary cause of death (Data-Field ID 40001) with any ICD10  
357 codes in the Chapter IX (Diseases of the circulatory system), which correspond to I00-I99 codes.  
358 Heart failure hospitalisation was defined as a hospitalisation at least 28 days after the first diagnosis,  
359 with the same code used for the heart failure patient definition. To match the modelling approach used  
360 in the clinical studies, the date of recruitment was used to calculate the time to event. The end of  
361 follow-up was considered to be the date of the last major UK Biobank update (01/09/2019).

362

363 **Exome-sequencing.** For CHARM, CORONA and UK Biobank, exomes were captured with the IDT  
364 xGen Exome Research Panel V1.0 (Integrated DNA Technologies, Coralville, IA, USA) and  
365 sequenced according to standard protocols on Illumina's NovaSeq 6000 (Illumina, San Diego, CA,  
366 USA) platform. Exome sequencing for CHARM and CORONA was performed using 150bp paired-  
367 end reads at the Institute for Genomic Medicine at the Columbia University Medical Center, as  
368 previously described<sup>14</sup>. Exome sequencing for the UK Biobank using 75-bp paired-end reads and  
369 initial sample-level QC the UK Biobank was performed at Regeneron Pharmaceuticals, as previously  
370 described<sup>14,43,44</sup>. Quality control of the genetic data performed by Regeneron included sex discordance,  
371 contamination, unresolved duplicated sequences and discordance with microarray genotyping data<sup>45</sup>.

372 Sequence data from all three studies was processed through the AstraZeneca's Centre for  
373 Genomics Research bioinformatics pipeline using a custom-built Amazon Web Services cloud  
374 compute platform running Illumina DRAGEN Bio-IT Platform Germline Pipeline v3.0.7. The reads  
375 were aligned to the GRCh38 genome reference, followed by single-nucleotide variant (SNV) and indel  
376 calling. SNVs and indels were first annotated using SnpEFF v4.34 against Ensembl Build 38.92.  
377 Variants were then annotated using the Genome Aggregation Database (gnomAD) minor allele  
378 frequencies (gnomAD v2.1.1 mapped to GRCh38), missense tolerance ratio (MTR) and REVEL  
379 scores<sup>46-48</sup>.

380

381 **Sample and variant quality control (QC).** The pre-QC dataset consisted of 3,090 CHARM, 2,906  
382 CORONA and 2,868 UK Biobank participants. The following samples were removed: discordance  
383 between self-reported sex and genomic predicted sex based on X:Y coverage ratio; >4%  
384 contamination according to VerifyBamID v1.0.5; <95% of CCDS (release 22) bases covered with at  
385 least 10-fold coverage; related (up to third degree with KING v2.2.3), probability of European  
386 Ancestry <0.98 (<0.99 for UK Biobank) based on PEDDY v0.4.2 predictions; and individuals within

387 four standard deviations of principal components 1-4 (**Supplementary Table 13**)<sup>49-51</sup>. The final  
388 filtered dataset for analysis consisted of 2,672 CHARM, 2,776 CORONA and 2,641 UK Biobank  
389 samples (**Figure 1, Table 1**).

390

391 **Gene-level collapsing analyses.** We first performed, in the three cohorts separately, gene-based  
392 collapsing analyses to identify patients carrying at least one qualifying variant in each protein-coding  
393 gene. A qualifying variant is defined as a variant that passes certain filter criteria specific to each  
394 genetic model. **Supplementary Table 14** summarises the genetic models used for the analyses. We  
395 analysed ten non-synonymous models (nine of which are dominant and one recessive), plus an  
396 additional synonymous variant model as a negative control<sup>52</sup>.

397 The data was modelled using Cox proportional hazards regression with Firth's penalized  
398 likelihood, which provides a solution to the non-convergence of the likelihood function, more  
399 frequently observed with rare-variant analysis: coxphf<sup>53,54</sup>. Genotypes were encoded as binary variable  
400 after the first step of collapsing analysis. The coxphf method has been shown to be appropriate for  
401 genome-wide time-to-event analysis, both in terms of controlling type I error rates, and power for  
402 variants with low minor allele frequency<sup>18</sup>. In CHARM and CORONA, age at recruitment, sex and  
403 treatment arm were used as covariates in all analyses. The coxphf default of confidence intervals and  
404 tests based on the profile penalized log likelihood was used. In the UK Biobank, age at recruitment  
405 (Data-Field ID 21022) and sex (Data-Field 22001) were used as covariates in all analyses. For the  
406 collapsing survival analysis, the Bonferroni multiplicity adjusted threshold was set at  $p=2.7 \times 10^{-7}$  ( $\alpha =$   
407  $[0.05 / (18,500 \text{ genes} * 10 \text{ non-synonymous models})]$ ). This threshold was supported by permuting the  
408 data using R perm function (n=1) within the synonymous model, comparing with observed p-values  
409 with quantile-quantile plots and estimating the genomic inflation factor  $\lambda$  (**Supplementary Fig. 5**).  
410 The proportionality of hazards assumption was examined for the top genes by using the Schoenfeld  
411 residuals against the transformed time.

412

413 **Meta-analysis.** We conducted a meta-analysis using PLINK v1.90 on the beta-values and standard  
414 errors extracted from the coxphf results. We computed both fixed and random effect meta-analysis  
415 models, and we only reported results supported by at least five carriers in each study. We computed  
416 both fixed and random effects meta-analysis models and reported random effects results with a  
417 heterogeneity index  $I^2 > 40$ . Consistent with the survival analysis, the meta-analysis Bonferroni  
418 multiplicity adjusted threshold was set at  $p < 2.7 \times 10^{-7}$  ( $\alpha = [0.05 / (18,500 \text{ genes} * 10 \text{ non-synonymous}$   
419  $\text{models})]$ ). Quantile-quantile plots for the meta-analysis were generated with (permutation-based)  
420 expected p-values from data permuted prior to the collapsing survival analysis using the R perm  
421 function (n=1) (**Supplementary Figs. 6A, 6B**).

422

423 **Sensitivity analysis.** Analyses were conducted with additional covariates such as BMI and prior  
424 diabetes to assess the robustness of results when relevant for the genes with significant results  
425 ( $p < 2.7 \times 10^{-7}$ ) in the meta-analysis of CHARM, CORONA and the UK Biobank for both tested  
426 outcomes. Detailed clinical information supporting the analyses are reported in **Table 1**. Sensitivity  
427 analyses did not change the observed results (**Supplementary Table 15**).

428

429 **RNA expression.** We interrogated median TPM-normalized gene expression for 54 tissues sampled in  
430 948 donors provided by GTEx v8<sup>27</sup>. We defined a subset of 16 cardiovascular tissues as follows:  
431 Adipose - Subcutaneous, Adipose - Visceral (Omentum), Adrenal Gland, Artery - Aorta, Artery -  
432 Coronary, Artery - Tibial, Heart - Atrial Appendage, Heart - Left Ventricle, Kidney - Cortex, Kidney -  
433 Medulla, Liver, Muscle - Skeletal, Pancreas, Spleen, Thyroid, Whole Blood.

434 In addition, we extracted and analysed data from three published myocardial transcriptomic  
435 analyses: (1) HFpEF (n=41), HFrEF (n=30) and controls (n=24); (2) DCM (n=166), HCM (n=28) and  
436 controls (n=166) (GSE141910, The Myocardial Applied Genomics Network;  
437 <https://www.med.upenn.edu/magnet/>); and (3) idiopathic DCM (n=82), ICM (n=95) and controls  
438 (n=136) (GSE57338)<sup>55</sup>.

439

440 **Annotation with GWAS data.** For the genes most significantly associated with heart failure  
441 progression, we compiled genetic evidence from the curated GWAS results of external studies  
442 available in the Cardiovascular Disease Knowledge Portal (<https://cvd.hugeamp.org/>). First, we listed  
443 the association with the lowest genome-wide significant p-values in the region, where associations are  
444 clumped by linkage disequilibrium and classified into three phenotypes group: cardiovascular, lipids  
445 and anthropometric. Then, we used the Cardiovascular Disease Knowledge Portal Genomic Region  
446 Miner tool to extract the lowest variant associations across each region or in the gene for the following  
447 six phenotypes: heart failure, non-ischemic cardiomyopathy, atrial fibrillation, any cardiovascular  
448 disease, myocardial infarction, or hypertension.

449

450 **Step-wise hypergeometric enrichment analysis with Mantis-ml.** Mantis-ml is a method for gene  
451 prioritisation, leveraging publicly available gene annotation data from multiple resources to derive  
452 genetic association scores for a user-specified disease<sup>25</sup>. Harnessing data from resources such as  
453 OMIM, ExAC, Essential Mouse Genes, GnomAD, MSigDB, GTEx and genic-intolerance scores  
454 (RVIS and MTR) among others, we used this tool to assess to what extent the most significant genes  
455 from the meta-analysis are similar to genes known to be associated with heart failure or  
456 cardiomyopathy.

457 We performed a step-wise hypergeometric test between the study-ranked list of genes with a fixed  
458 p-value < 0.01 for one of the outcomes (**Supplementary Tables 11, 12**) and 18,626 genes pre-ranked  
459 by their Mantis-ml association scores for 33 diseases containing either ‘heart failure’ or

460 ‘cardiomyopathy’ (i.e., 26 from OpenTargets, four from HPO, three from Genomics England). An  
461 overview of these diseases is provided in **Supplementary Table 16**. The resulting step-wise  
462 hypergeometric curves are shown in **Supplementary Fig. 1**.

463 This test quantifies the overlap between the list of genes identify in this heart failure progression  
464 study and the list of genes ranked according to independent data sources by Mantis-ml. The p-values  
465 generated are converted to Phred scores. Enrichment performance were assessed and p-values  
466 obtained using the one-sided Mann-Whitney U test.

467

468 **Gene ontology enrichment analysis.** A functional enrichment analysis was performed using  
469 g:Profiler for the same lists of genes ordered on fixed p-value as done for the annotation with Mantis-  
470 ml, i.e., the genes with a fixed effect p-value<0.01 for each of the outcomes (**Supplementary Tables**  
471 **11, 12**)<sup>56</sup>. The data sources tested were Gene Ontology (GO, molecular function, cellular component,  
472 biological process), KEGG and miRTarBase. The background set of gene used to compute the  
473 functional enrichment was the 18,948 genes list from the Consensus Coding Sequence (CCDS, release  
474 22), over annotated genes. Multiple testing correction for p-values was computed by applying the  
475 default g:SCS method.

476

477 **Tractability assessment.** For the genes most significantly associated with heart failure progression,  
478 we assessed the amenability to intervention by different drug modalities, including small molecules,  
479 antibodies, PROTAC and others, using the Open Target Platform (<https://platform.opentargets.org/>).  
480 The genes were categorized based on ‘buckets’ representing different levels of tractability, ranging  
481 from high confidence (lower number) to uncertain tractability (higher number), as previously  
482 described<sup>57</sup>. In addition, genes were also classified according to their ‘target development level’ (TDL)  
483 into either of four classes (i.e., Tclin, Tchem, Tbio or Tdark) using the Target Central Resource  
484 Database (TCRD, <http://juniper.health.unm.edu/tcrd/>). In brief, Tclin are proteins through which  
485 approved drugs act (i.e., mode-of-action drug targets); Tchem are proteins known to bind small  
486 molecules with high potency; Tbio are proteins with well-studied biology, having a fractional  
487 publication count above 5; and Tdark are understudied proteins that do not meet criteria for the above  
488 3 categories, respectively (**Supplementary Table 10**).

489

490 **Co-expression network analysis.** To further explore the *CUTC* function, we performed co-expression  
491 analysis using GeneNetwork v2.0 (<https://www.genenetwork.nl/>), which predicts pathway and human  
492 phenotype associations using 31,499 public human RNA-seq samples (**Supplementary Fig. 4**).<sup>58</sup>

493

494

495 **Data availability**

496

497 Summary statistics from the rare-variant collapsing analyses are available within the article and its  
498 Supplementary Information files. Access to the UK Biobank data can be gained via the UK Biobank  
499 website: <https://bbams.ndph.ox.ac.uk/ams/>.

500

501

## 502 Code availability

503

504 Sequence data were processed through a custom-built Amazon Web Services cloud compute platform  
505 running Illumina DRAGEN Bio-IT Platform. SNVs and indels were annotated using SnpEFF v4.3  
506 against Ensembl v38.92. The software used in this study are referenced in the manuscript and are  
507 available online: Mantis-ml (<https://github.com/astrazeneca-cgr-publications/mantis-ml-release>),  
508 QQperm (<https://cran.r-project.org/web/packages/QQperm/index.html>).

509

510

## 511 References

- 512 1 GBD 2017 Disease and Injury Incidence and Prevalence Collaborators. Global, regional, and  
513 national incidence, prevalence, and years lived with disability for 354 diseases and injuries for  
514 195 countries and territories, 1990-2017: a systematic analysis for the Global Burden of  
515 Disease Study 2017. *Lancet* **392**, 1789-1858 (2018).
- 516 2 Metra, M. & Teerlink, J. R. Heart failure. *Lancet* **390**, 1981-1995 (2017).
- 517 3 McMurray, J. J. V. & Pfeffer, M. A. Heart failure. *Lancet* **365**, 1877-1889 (2005).
- 518 4 Dickstein, K. *et al.* ESC Guidelines for the diagnosis and treatment of acute and chronic heart  
519 failure 2008: the Task Force for the Diagnosis and Treatment of Acute and Chronic Heart  
520 Failure 2008 of the European Society of Cardiology. Developed in collaboration with the  
521 Heart Failure Association of the ESC (HFA) and endorsed by the European Society of  
522 Intensive Care Medicine (ESICM). *Eur Heart J* **29**, 2388-2442 (2008).
- 523 5 Cook, C., Cole, G., Asaria, P., Jabbour, R. & Francis, D. P. The annual global economic  
524 burden of heart failure. *Int J Cardiol* **171**, 368-376 (2014).
- 525 6 Savarese, G. & Lund, L. H. Global Public Health Burden of Heart Failure. *Card Fail Rev* **3**, 7-  
526 11 (2017).
- 527 7 Retrum, J. H. *et al.* Patient-identified factors related to heart failure readmissions. *Circ*  
528 *Cardiovasc Qual Outcomes* **6**, 171-177 (2013).
- 529 8 Roger, V. L. *et al.* Heart disease and stroke statistics--2012 update: a report from the  
530 American Heart Association. *Circulation* **125**, e2-e220 (2012).
- 531 9 National Clinical Guideline Centre (UK). *Chronic Heart Failure: National Clinical Guideline*  
532 *for Diagnosis and Management in Primary and Secondary Care: Partial Update*. (Royal  
533 College of Physicians (UK), 2010).
- 534 10 Lindgren, M. P. *et al.* A Swedish Nationwide Adoption Study of the Heritability of Heart  
535 Failure. *JAMA cardiology* **3**, 703-710 (2018).
- 536 11 Shah, S. *et al.* Genome-wide association and Mendelian randomisation analysis provide  
537 insights into the pathogenesis of heart failure. *Nature Communications* **11**, 163 (2020).
- 538 12 Arvanitis, M. *et al.* Genome-wide association and multi-omic analyses reveal ACTN2 as a  
539 gene linked to heart failure. *Nature Communications* **11**, 1122 (2020).
- 540 13 Joseph, J. *et al.* Genetic Architecture of Heart Failure with Preserved versus Reduced Ejection  
541 Fraction. *medRxiv*, 2021.2012.2001.21266829 (2021).
- 542 14 Povysil, G. *et al.* Assessing the Role of Rare Genetic Variation in Patients With Heart Failure.  
543 *JAMA Cardiol* **6**, 379-386 (2021).

- 544 15 Cox, D. R. Regression Models and Life-Tables. *Journal of the Royal Statistical Society: Series B (Methodological)* **34**, 187-202 (1972).  
545  
546 16 Xue, X. *et al.* Testing the proportional hazards assumption in case-cohort analysis. *BMC Med Res Methodol* **13**, 88 (2013).  
547  
548 17 Li, R. *et al.* Fast Lasso method for large-scale and ultrahigh-dimensional Cox model with applications to UK Biobank. *Biostatistics* **23**, 522-540 (2022).  
549  
550 18 Bi, W., Fritsche, L. G., Mukherjee, B., Kim, S. & Lee, S. A Fast and Accurate Method for Genome-Wide Time-to-Event Data Analysis and Its Application to UK Biobank. *American Journal of Human Genetics* **107**, 222-233 (2020).  
551  
552 19 Legault, M.-A., Perreault, L.-P. L. & Dubé, M.-P. ExPheWas: a browser for gene-based pheWAS associations. *medRxiv*, 2021.2003.2017.21253824 (2021).  
553  
554 20 Lumbers, R. T. *et al.* The genomics of heart failure: design and rationale of the HERMES consortium. *ESC Heart Fail* **8**, 5531-5541 (2021).  
555  
556 21 Povysil, G. *et al.* Rare-variant collapsing analyses for complex traits: guidelines and applications. *Nat Rev Genet* **20**, 747-759 (2019).  
557  
558 22 Pfeffer, M. A. *et al.* Effects of candesartan on mortality and morbidity in patients with chronic heart failure: the CHARM-Overall programme. *Lancet* **362**, 759-766 (2003).  
559  
560 23 Kjekshus, J. *et al.* Rosuvastatin in older patients with systolic heart failure. *N Engl J Med* **357**, 2248-2261 (2007).  
561  
562 24 Bycroft, C. *et al.* The UK Biobank resource with deep phenotyping and genomic data. *Nature* **562**, 203-209 (2018).  
563  
564 25 Vitsios, D. & Petrovski, S. Mantis-ml: Disease-Agnostic Gene Prioritization from High-Throughput Genomic Screens by Stochastic Semi-supervised Learning. *American Journal of Human Genetics* **106**, 659-678 (2020).  
565  
566 26 Tobita, T. *et al.* Genetic basis of cardiomyopathy and the genotypes involved in prognosis and left ventricular reverse remodeling. *Sci Rep* **8**, 1998 (2018).  
567  
568 27 Consortium, G. T. The GTEx Consortium atlas of genetic regulatory effects across human tissues. *Science* **369**, 1318-1330 (2020).  
569  
570 28 Hahn, V. S. *et al.* Myocardial Gene Expression Signatures in Human Heart Failure With Preserved Ejection Fraction. *Circulation* **143**, 120-134 (2021).  
571  
572 29 Worman, H. J., Ostlund, C. & Wang, Y. Diseases of the nuclear envelope. *Cold Spring Harb Perspect Biol* **2**, a000760 (2010).  
573  
574 30 Wittemans, L. B. L. *et al.* Assessing the causal association of glycine with risk of cardiometabolic diseases. *Nature Communications* **10**, 1060 (2019).  
575  
576 31 Li, Y., Du, J., Zhang, P. & Ding, J. Crystal structure of human copper homeostasis protein CutC reveals a potential copper-binding site. *J Struct Biol* **169**, 399-405 (2010).  
577  
578 32 Gupta, S. D., Lee, B. T., Camakaris, J. & Wu, H. C. Identification of cutC and cutF (nlpE) genes involved in copper tolerance in Escherichia coli. *J Bacteriol* **177**, 4207-4215 (1995).  
579  
580 33 Li, J. *et al.* Identification and characterization of a novel Cut family cDNA that encodes human copper transporter protein CutC. *Biochem Biophys Res Commun* **337**, 179-183 (2005).  
581  
582 34 Liu, Y. & Miao, J. An Emerging Role of Defective Copper Metabolism in Heart Disease. *Nutrients* **14** (2022).  
583  
584 35 Uchiumi, F., Fujikawa, M., Miyazaki, S. & Tanuma, S.-i. Implication of bidirectional promoters containing duplicated GGAA motifs of mitochondrial function-associated genes. *AIMS Mol Sci* **1**, 1-26 (2014).  
585  
586 36 Berridge, M. J., Bootman, M. D. & Roderick, H. L. Calcium signalling: dynamics, homeostasis and remodelling. *Nat Rev Mol Cell Biol* **4**, 517-529 (2003).  
587  
588 37 Rinnier, R. T., Goldberg, M. E. & Torjman, M. C. in *The Essence of Analgesia and Analgesics* (eds J. Michael Watkins-Pitchford, Jonathan S. Jahr, & Raymond S. Sinatra) 310-315 (Cambridge University Press, 2010).  
589  
590 38 Suckfüll, M. *et al.* A randomized, double-blind, placebo-controlled clinical trial to evaluate the efficacy and safety of neramexane in patients with moderate to severe subjective tinnitus. *BMC Ear Nose Throat Disord* **11**, 1 (2011).  
591  
592 39 Sueta, D., Tabata, N. & Hokimoto, S. Clinical roles of calcium channel blockers in ischemic heart diseases. *Hypertens Res* **40**, 423-428 (2017).  
593  
594  
595  
596  
597  
598



- 599 40 Yndestad, A. *et al.* Role of inflammation in the progression of heart failure. *Curr Cardiol Rep*  
600 **9**, 236-241 (2007).
- 601 41 Dick, S. A. & Epelman, S. Chronic Heart Failure and Inflammation: What Do We Really  
602 Know? *Circ Res* **119**, 159-176 (2016).
- 603 42 Bloxham, C. J., Foster, S. R. & Thomas, W. G. A Bitter Taste in Your Heart. *Front Physiol*  
604 **11**, 431 (2020).
- 605 43 Wang, Q. *et al.* Rare variant contribution to human disease in 281,104 UK Biobank exomes.  
606 *Nature* **597**, 527-532 (2021).
- 607 44 Szustakowski, J. D. *et al.* Advancing human genetics research and drug discovery through  
608 exome sequencing of the UK Biobank. *Nat Genet* **53**, 942-948 (2021).
- 609 45 Van Hout, C. V. *et al.* Exome sequencing and characterization of 49,960 individuals in the UK  
610 Biobank. *Nature* **586**, 749-756 (2020).
- 611 46 Ioannidis, N. M. *et al.* REVEL: An Ensemble Method for Predicting the Pathogenicity of Rare  
612 Missense Variants. *Am J Hum Genet* **99**, 877-885 (2016).
- 613 47 Traynelis, J. *et al.* Optimizing genomic medicine in epilepsy through a gene-customized  
614 approach to missense variant interpretation. *Genome Res* **27**, 1715-1729 (2017).
- 615 48 Karczewski, K. J. *et al.* The mutational constraint spectrum quantified from variation in  
616 141,456 humans. *Nature* **581**, 434-443 (2020).
- 617 49 Pedersen, B. S. & Quinlan, A. R. Who's Who? Detecting and Resolving Sample Anomalies in  
618 Human DNA Sequencing Studies with Peddy. *American Journal of Human Genetics* **100**,  
619 406-413 (2017).
- 620 50 Jun, G. *et al.* Detecting and estimating contamination of human DNA samples in sequencing  
621 and array-based genotype data. *American Journal of Human Genetics* **91**, 839-848 (2012).
- 622 51 Manichaikul, A. *et al.* Robust relationship inference in genome-wide association studies.  
623 *Bioinformatics (Oxford, England)* **26**, 2867-2873 (2010).
- 624 52 Carss, K. J. *et al.* Spontaneous Coronary Artery Dissection: Insights on Rare Genetic  
625 Variation From Genome Sequencing. *Circ Genom Precis Med* **13**, e003030 (2020).
- 626 53 Heinze, G. & Schemper, M. A solution to the problem of monotone likelihood in Cox  
627 regression. *Biometrics* **57**, 114-119 (2001).
- 628 54 Dunkler, D., Ploner, M., Schemper, M. & Heinze, G. Weighted Cox Regression Using the R  
629 Package *coxphw*. *J. Stat. Soft.* **84**, 1-26 (2018).
- 630 55 Liu, Y. *et al.* RNA-Seq identifies novel myocardial gene expression signatures of heart failure.  
631 *Genomics* **105**, 83-89 (2015).
- 632 56 Raudvere, U. *et al.* g:Profiler: a web server for functional enrichment analysis and conversions  
633 of gene lists (2019 update). *Nucleic Acids Research* **47**, W191-W198 (2019).
- 634 57 Brown, K. K. *et al.* Approaches to target tractability assessment - a practical perspective.  
635 *Medchemcomm* **9**, 606-613 (2018).
- 636 58 Deelen, P. *et al.* Improving the diagnostic yield of exome- sequencing by predicting gene-  
637 phenotype associations using large-scale gene expression analysis. *Nat Commun* **10**, 2837  
638 (2019).
- 639 59 Cochran, W. G. The Combination of Estimates from Different Experiments. *Biometrics* **10**,  
640 101-129 (1954).
- 641 60 Higgins, J. P. T. & Thompson, S. G. Quantifying heterogeneity in a meta-analysis. *Stat Med*  
642 **21**, 1539-1558 (2002).
- 643 61 Cerami, E. *et al.* The cBio cancer genomics portal: an open platform for exploring  
644 multidimensional cancer genomics data. *Cancer Discov* **2**, 401-404 (2012).
- 645 62 Gao, J. *et al.* Integrative analysis of complex cancer genomics and clinical profiles using the  
646 cBioPortal. *Sci Signal* **6**, pl1 (2013).

647

648

649 **Acknowledgments**

650

651 We thank the participants and investigators of the UK Biobank study who made this work possible  
652 (Resource Application Number 26041). We thank the UKB Exome Sequencing Consortium (UKB-  
653 ESC) members AbbVie, Alnylam Pharmaceuticals, AstraZeneca, Biogen, Bristol-Myers Squibb,  
654 Pfizer, Regeneron and Takeda for funding the generation of the data, and the Regeneron Genetics  
655 Center for completing the sequencing and initial quality control of the exome sequencing data. We  
656 acknowledge the AstraZeneca Centre for Genomics Research Analytics and Informatics team for  
657 processing and analysis of sequencing data. We thank all the study participants for contributing to this  
658 effort and the CHARM and CORONA co-investigators. Finally, we thank Sri Deevi and Dorota  
659 Matelska from the AstraZeneca Centre for Genomics Research for their support, for which we are  
660 grateful. M.-P.D. is funded by the Canada Research Chairs Program and by the Health Collaboration  
661 Acceleration Fund from the Government of Quebec. J.C.T. holds the Canada Research Chair in  
662 personalized and translational medicine and the Université de Montréal endowed research chair in  
663 atherosclerosis.

664

665

666 **Author Contributions Statement**

667

668 O.C., M-P.D., C.H., J-C.T., D.S.P. and K.C. conceived and designed the study. O.C., Q.W., L.M. and  
669 A.W. performed the statistical and computational analyses. M-P.D., D.V., D.S.P. and K.C. supervised  
670 the analyses. M-P.D., C.B.G, J.K., C.H., J-C.T., D.S.P. and K.C. participated in the acquisition of the  
671 data. O.C., M-P.D., Q.W., L.M., D.V., A.W., Q-D.W., K.M.H., C.B.G, J.K., C.H., J-C.T., D.S.P. and  
672 K.C. participated in the data interpretation. O.C., M-P.D., L.M., A.W., J-C.T., D.S.P. and K.C. wrote  
673 the initial draft of the manuscript. All authors contributed to the revision of the first draft. All authors  
674 approved the final version of the manuscript.

675

676

677 **Competing Interests Statement**

678

679 O.C., Q.W., L.M., D.V., A.W., Q.-D.W., K.M.H., C.H., D.S.P. and K.C. report personal fees from  
680 AstraZeneca during the conduct of the study. Q.W., C.H. and D.S.P. are stockholders of AstraZeneca.  
681 M.-P.D. reports personal fees and minor equity interest from Dalcor, other from AstraZeneca,  
682 GlaxoSmithKline, Pfizer, Servier, Sanofi. J.C.T. reports a grant from AstraZeneca for the conduct of  
683 the study; other grants from AstraZeneca, Ceapro, DalCor Pharmaceuticals, Esperion, Ionis, Novartis,  
684 Pfizer and RegenXBio; honoraria from AstraZeneca, DalCor Pharmaceuticals, HLS Pharmaceuticals,

685 Pendopharm and Pfizer; minor equity interest in DalCor Pharmaceuticals. J.C.T. is author on patents  
686 “Methods of treating a coronavirus infection using Colchicine and Methods of treating a coronavirus  
687 infection using Colchicine” pending and a patent “Early administration of low-dose colchicine after  
688 myocardial infarction” pending assigned to the Montreal Heart Institute. M.-P.D. and J.C.T. are  
689 authors on a patent “Methods for Treating or Preventing Cardiovascular Disorders and Lowering Risk  
690 of Cardiovascular Events” issued to Dalcor, no royalties received, a patent “Genetic Markers for  
691 Predicting Responsiveness to Therapy with HDL-Raising or HDL Mimicking Agent” issued to  
692 Dalcor, no royalties received, and a patent “Methods for using low dose colchicine after myocardial  
693 infarction”, assigned to the Montreal Heart Institute. J.C.T. has waived his rights in colchicine patents  
694 and does not stand to gain financially. C.B.G. reports personal fees from AbbVie, Bayer, Boston  
695 Scientific, CeleCor, Correvio, Espero BioPharma, Medscape, Medtronic, Merck, National Institutes of  
696 Health, Novo Nordisk, Rhoshan and Roche; grants from Akros, Apple, AstraZeneca, Daiichi Sankyo,  
697 US Food and Drug Administration, GlaxoSmithKline and Medtronic Foundation; grants and personal  
698 fees from Boehringer Ingelheim, Bristol Myers Squibb, Janssen, Novartis and Pfizer; and other  
699 support from Duke Clinical Research Institute outside the submitted work. Funding for the exome  
700 sequencing in the CHARM, CORONA and UK Biobank studies was provided fully or partially by  
701 AstraZeneca.  
702

703 **Tables**

704

705 **Table 1. Characteristics of patients included in the analysis.**

706

	<b>CHARM</b>	<b>CORONA</b>	<b>UK Biobank</b>	<b>Total</b>
<b>Number of patients, n</b>	2,672	2,776	2,641	8,089
<b>Age, mean ± SD</b>	66.5 ± 10.9	72.5 ± 6.9	61.9 ± 6.1	67.1 ± 9.3
<b>Men, n (%)</b>	1,788 (66.9%)	2,139 (77.1%)	2,016 (76.3%)	5,943 (73.5%)
<b>Treatment (interventional)</b>	1,346 (50.4%)	1,391 (50.1%)	NA	NA
<b>LVEF, mean ± SD</b>	0.38 ± 0.15	0.31 ± 0.06	NA*	0.35 ± 0.12
<b>BMI (kg/m<sup>2</sup>), mean ± SD</b>	28.6 ± 5.8	27.4 ± 4.5	30.2 ± 5.6	28.7 ± 5.4
<b>Current smoker, n (%)</b>	384 (14.4%)	250 (9.0%)	334 (12.6%)	968 (12.0%)
<b>Myocardial infarction, n (%)</b>	1,490 (55.8%)	1,692 (61.0%)	1,312 (49.7%)	4,494 (55.6%)
<b>Diabetes, n (%)</b>	768 (28.7%)	763 (27.5%)	850 (32.2%)	2,381 (29.4%)
<b>Atrial fibrillation, n (%)</b>	801 (30.0%)	1,931 (69.6%)	1,260 (47.7%)	3,992 (49.4%)
<b>CV death</b>	504 (18.9%)	358 (12.9%)	466 (17.6%)	1,328 (16.4%)
<b>CV death and/or HF hospitalisation</b>	895 (33.5%)	843 (30.4%)	713 (27.0%)	2,451 (30.3%)

707

708 \*LVEF only available for 66 UK Biobank individuals. BMI: body mass index; CV: cardiovascular; HF: heart  
709 failure; LVEF: left ventricular ejection fraction; N: number of patients; NA: not available; SD: standard  
710 deviation.

711

**Table 2. Gene-based collapsing meta-analysis results for ‘time to cardiovascular death’ (top) or ‘time to cardiovascular death and/or hospitalisation for heart failure’ (bottom).**

Gene	Genetic model*	N (studies)	P	HR (95% CI)	SE	Q	I <sup>2</sup> **	Total N (carriers)	CHARM P (carriers) <sup>†</sup>	CORONA P (carriers) <sup>†</sup>	UK Biobank P (carriers) <sup>†</sup>
<b>Time to cardiovascular death</b>											
<i>FAM221A</i>	Flexible non-synonymous	3	3.85E-08	5.14 (2.87, 9.21)	1.35	0.20	38.02	25	1.38E-02 (8)	6.48E-01 (7)	1.77E-04 (10)
<i>CUTC</i>	Flexible non-synonymous (MTR)	3	3.90E-08	5.13 (2.85, 9.13)	1.35	0.50	0	19	1.67E-02 (5)	1.70E-01 (6)	6.32E-04 (8)
<i>IFIT5</i>	Flexible damaging	3	4.77E-08	4.77 (2.72, 8.33)	1.34	0.36	2.20	24	2.47E-02 (8)	9.19E-04 (8)	5.91E-02 (8)
<i>STIMATE</i>	Flexible non-synonymous	3	7.68E-08	4.39 (2.56, 7.52)	1.32	0.50	0	25	4.28E-02 (6)	8.69E-04 (10)	4.28E-02 (9)
<i>TAS2R20</i>	Flexible non-synonymous, Flexible non-synonymous (MTR)	3	2.57E-07	3.93 (2.34, 6.63)	1.31	0.26	25.85	34	3.44E-02 (10)	1.54E-04 (16)	7.69E-01 (8)
<b>Time to cardiovascular death and/or hospitalisation for heart failure</b>											
<i>CALB2</i>	Flexible non-synonymous	3	4.82E-09	4.47 (2.71, 7.39)	1.30	0.20	37.83	21	6.94E-02 (8)	3.05E-02 (6)	1.07E-04 (7)
<i>BLK</i>	Ultra-rare	2	5.46E-08	6.88 (3.43, 13.84)	1.43	0.86	0	10	NA	1.49E-03 (5)	7.67E-03 (5)

Fixed-effects meta-analysis p-value <  $2.7 \times 10^{-7}$ ; \*genetic model details in **Supplementary Table 14**; \*\*filtered on  $I^2 \leq 40$ ; <sup>†</sup>filtered on carrier count  $\geq 5$  from input (a posteriori); P: Fixed-effects meta-analysis p-value; HR: hazard ratio; CI: confidence interval; SE: standard error; Q: Cochran’s Q p-value testing for heterogeneity<sup>59</sup>;  $I^2$ : percentage of variation across studies that is due to heterogeneity rather than chance<sup>60</sup>; CHARM/CORON/UK Biobank P: coxphf p-value for CHARM/CORONA/UK Biobank; MTR, missense tolerance ratio.

**Table 3. Summary of supporting genetic evidence from (A) Cardiovascular Disease Knowledge Portal and (B) published GWAS on several cardiovascular outcomes.**

Gene	A) Cardiovascular Disease Knowledge Portal									B) Published GWAS data											
	Cardiovascular			Lipids			Anthropometric			Heart failure		Non-ischemic cardiomyopathy		Atrial fibrillation		Any cardiovascular disease		Myocardial infarction		Hypertension	
	Trait	P	beta	Trait	P	beta	Trait	P	beta	P	beta	P	beta	P	beta	P	beta	P	beta	P	beta
<i>FAM221A</i>							Height	3.52E-76	▼-0.0007	1.29E-04	▲1.06	5.03E-02	▲1.07	8.76E-05	▲5.82	1.71E-04	▲1.04	9.32E-03	▲3.38	4.57E-03	▲1.02
<i>CUTC</i>	Heart rate	2.73E-09	▼-0.100				Height	1.80E-28	▼-0.0003	1.67E-03	▲1.86	8.07E-03	▼0.85	1.79E-04	▲1.52	6.82E-03	▼0.95	1.25E-02	▲13.52	2.20E-05	▼0.95
<i>IFIT5</i>	Diastolic blood pressure	1.74E-08	▲0.011							2.72E-03	▲2.59	2.37E-03	▼0.81	1.76E-03	▲1.20	2.32E-06	▲1.02	1.62E-02	▼0.08	1.38E-04	▲1.23
<i>STIMATE</i>	Pulse pressure	1.03E-13	▲0.007	TGs	8.92E-19	▼-0.023	Height	8.09E-83	▼-0.0006	2.08E-03	▲1.04	1.27E-04	▲1.20	5.00E-03	▲2.16	1.00E-07	▼0.95	7.35E-04	▲1.17	6.26E-06	▲1.02
<i>TAS2R20</i>										2.21E-03	▲1.07	1.77E-03	▲1.50	4.28E-03	▲1.73	6.80E-03	▼0.99	2.74E-02	▼0.86	4.19E-03	▼0.86
<i>CALB2</i>	Ascending aorta diameter	2.90E-34	▼-0.190	LDL-C	2.57E-292	▲0.033	BMI	2.42E-22	▼-0.020	1.34E-03	▲1.04	2.22E-03	▼0.84	8.40E-04	▲1.37	1.22E-04	▼0.96	3.81E-02	▼0.85	3.20E-06	▼0.96
<i>BLK</i>	Systolic blood pressure	2.07E-22	▼-0.013	TGs	9.71E-30	▲0.027	BMI	1.20E-25	▼-0.012	7.22E-04	▼0.94	2.72E-03	▼0.85	6.31E-03	▲1.29	1.84E-03	▲1.02	1.27E-03	▲48.34	6.14E-05	▲1.05

From the Cardiovascular Disease Knowledge Portal, we retrieved the most significant common-variant associations ( $p \leq 5 \times 10^{-8}$ ) for cardiovascular, lipid and anthropometric traits at each gene region, clumped by linkage disequilibrium.

## Figures

Figure 1. Study design.

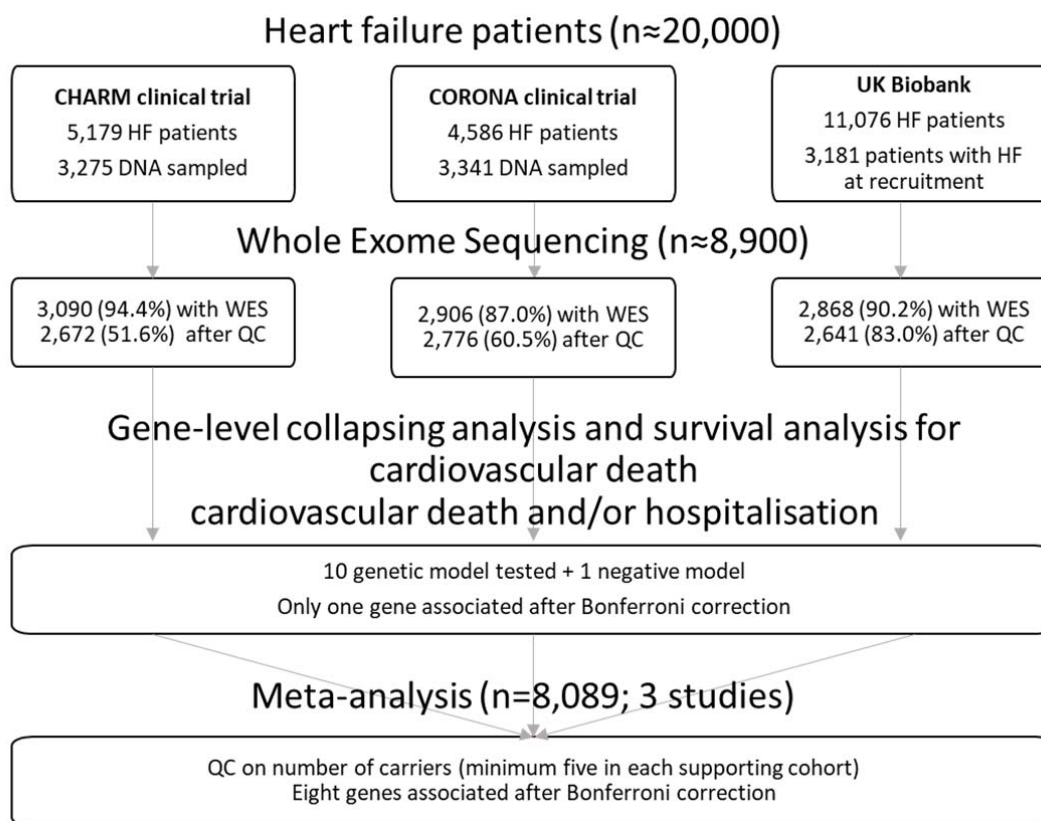
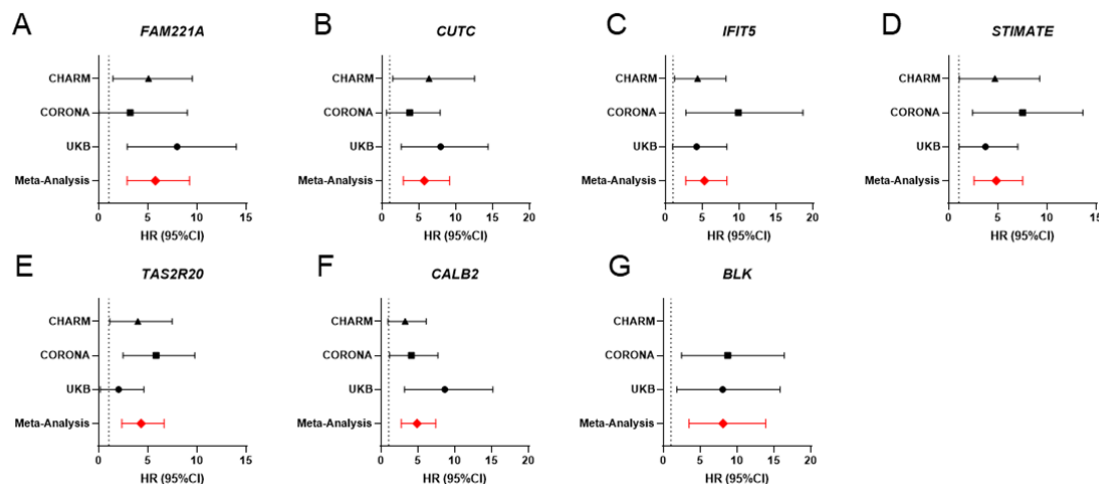


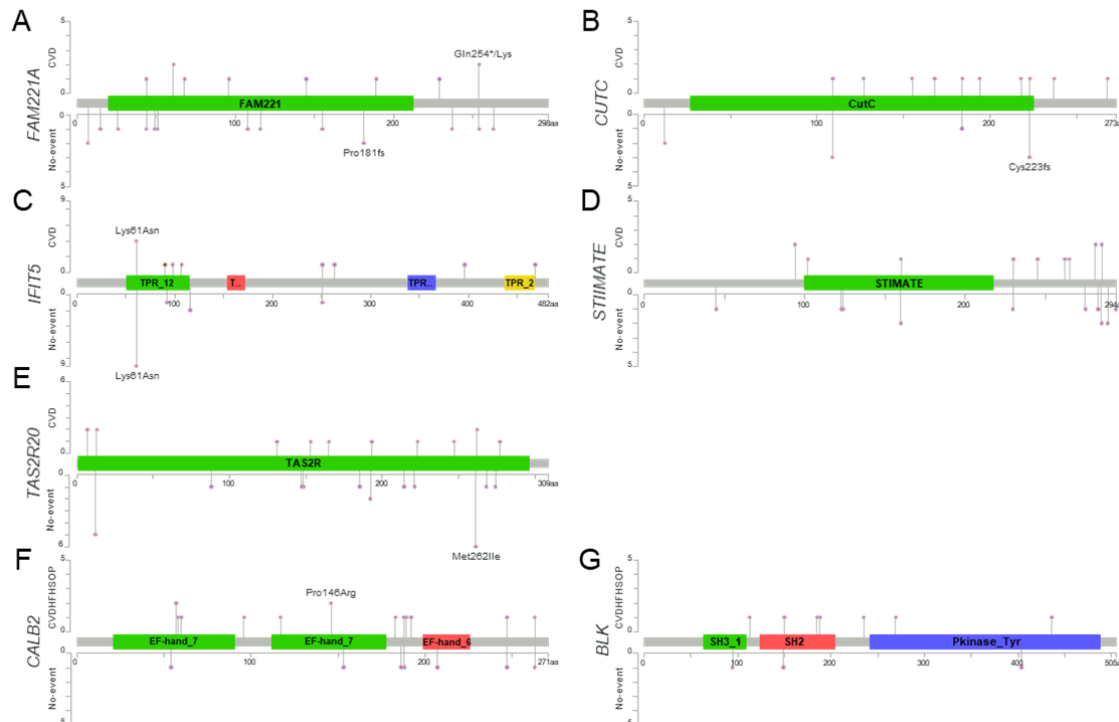
**Figure 2. Forest plot of the significant results ( $p < 2.7 \times 10^{-7}$ ) from the meta-analysis of CHARM, CORONA and the UK Biobank for time to cardiovascular death (A-E) and time to cardiovascular death and/or hospitalisation for heart failure (F-G).**



**A**, *FAM221A* in the flexible non-synonymous model; **B**, *CUTC* in the flexible non-synonymous (MTR) model; **C**, *IFIT5* in the flexible damaging model; **D**, *STIMATE* in the flexible non-synonymous model; **E**, *TAS2R20* in the flexible non-synonymous and/or in flexible non-synonymous (MTR) model; **F**, *CALB2* in the flexible non-synonymous model; **G**, *BLK* in the ultra-rare model.



**Figure 3. Lollipop plots depicting the individual variants across the candidate genes from the meta-analysis of time to cardiovascular death (A-E) and time to cardiovascular death and/or hospitalisation for heart failure (F-G).**



Variants in patients with event at the top and no-event at the bottom. More details on variants identified in heart failure patients with detrimental events in **Supplementary Table 4**. **A**, *FAM221A* in the flexible non-synonymous model (ENST00000344962); **B**, *CUTC* in the flexible non-synonymous (MTR) model (ENST00000370476); **C**, *IFIT5* in the flexible damaging model (ENST00000371795); **D**, *STIMATE* in the flexible non-synonymous model (ENST00000355083); **E**, *TAS2R20* in the flexible non-synonymous and/or in flexible non-synonymous (MTR) model (ENST00000538986); **F**, *CALB2* in the flexible non-synonymous model (ENST00000302628); **G**, *BLK* in the ultra-rare model (ENST00000259089). Lollipop plots were produced with the cbiportal mutation mapper tool<sup>61,62</sup>.

**Figure 4. Heatmaps showing the differential expression in cardiac tissue from patients with heart failure vs controls of candidate genes from the meta-analysis of time to cardiovascular death and time to cardiovascular death and/or hospitalisation for heart failure. The heatmaps show **A**, magnitude of change (log<sub>2</sub>FC; red: upregulated in HF vs control; blue: downregulated in HF vs control), and **B**, significance (-log<sub>10</sub>(adj. p-value)). ns: not significant (adj. p>0.05), na: not assessed.**

